A Generalized Constraint Model for Two-Dimensional Beam Flexures: Nonlinear Strain Energy Formulation

Shorya Awtar[1]
e-mail: awtar@umich.edu

Shiladitya Sen
e-mail: shiladit@umich.edu

Department of Mechanical Engineering,
University of Michigan,
2350 Hayward Street,
Ann Arbor, MI 48109

The beam constraint model (BCM), presented previously, captures pertinent nonlinearities to predict the constraint characteristics of a generalized beam flexure in terms of its stiffness and error motions. In this paper, a nonlinear strain energy formulation for the beam flexure, consistent with the transverse-direction load-displacement and axial-direction geometric constraint relations in the BCM, is presented. An explicit strain energy expression, in terms of beam end displacements, that accommodates generalized loading conditions, boundary conditions, initial curvature, and beam shape, is derived. Using energy-based arguments, new insight into the BCM is elucidated by fundamental relations among its stiffness, constraint, and energy coefficients. The presence of axial load in the geometric constraint and strain energy expressions—a unique attribute of distributed compliance flexures that leads to the elastokinematic effect—is highlighted. Using the principle of virtual work, this strain energy expression for a generalized beam is employed in determining the load-displacement relations, and therefore constraint characteristics, of a flexure mechanism comprising multiple beams. The benefit of this approach is evident in its mathematical efficiency and succinctness, which is to be expected with the use of energy methods. All analytical results are validated to a high degree of accuracy via nonlinear finite element analysis. [DOI: 10.1115/1.4002006]

Keywords: nonlinear strain energy, beam flexure, beam constraint model, beam characteristic coefficients, elastokinematic effect, nonlinear beam mechanics, flexure mechanisms

1 Introduction and Background

The beam constraint model (BCM) is a closed-form, parametric, and generalized model that captures the constraint characteristics of a beam flexure in terms of its stiffness and error motions. While the background and motivation for this model are presented in a preceding paper [1], a brief review is provided in the following paragraphs.

Figure 1 illustrates a simple beam (initially straight, uniform cross section) of length L, thickness T, and depth H, interconnecting rigid bodies (1) and (2). The beam is subject to generalized end loads $\boldsymbol{F_{XL}}$, $\boldsymbol{F_{YL}}$, and $\boldsymbol{M_{ZL}}$, which result in end displacements U_{XL}, U_{YL}, and θ_{ZL} with respect to the coordinate frame X-Y-Z. Transverse-direction displacements U_{YL} and θ_{ZL} can be recognized to be the degrees of freedom (DoF) of this flexure unit, while the axial-direction displacement U_{XL} represents a degree of constraint (DoC).

The BCM, expressed in terms of the transverse-direction end load-displacement relation and the axial-direction geometric constraint relation for the above beam flexure, has been derived previously [1,2]. It captures the nonlinearities associated with applying load equilibrium in the deformed state but neglects those associated with beam curvature. It has been shown that the former are crucial in accurately capturing the constraint characteristics of a beam flexure in terms of its stiffness and error motions over a practical range of loads and displacements. The BCM has also been extended to include beams with a wide range of end loads, initial and boundary conditions, and beam shapes. Furthermore, it has been employed to accurately determine the load-displacement relations, and therefore constraint characteristics, of more complex flexure mechanisms that comprise beam flexures [3,4]. However, the direct application of the BCM for this purpose proves to be mathematically tedious since all the internal loads and displacements associated with each beam have to be taken into account.

This limitation provides the motivation for the energy-based formulation of the BCM presented in this paper. In particular, the principle of virtual work (PVW) is employed because it eliminates the need to consider internal loads and load equilibrium for each constituent beam in a flexure mechanism [5]. The first requirement for applying PVW on an elastic system is the determination of the strain energy corresponding to an arbitrary deformed state. This is nontrivial because we want to capture a certain class of nonlinearities in the BCM while neglecting others. Furthermore, the assumptions in the strain energy formulation have to be consistent with those made in the direct determination of the transverse and axial relations in the BCM. This is addressed in Sec. 2 of this paper, where nonlinear strain and strain energy expressions are developed.

In Sec. 3, we derive expressions for the transverse-direction load-displacement relation, axial-direction geometric constraint relation, and total strain energy explicitly in terms of the end loads and end displacements for a variable cross-section beam. Upon simplification (series expansion and truncation), these three expressions reveal *beam characteristic coefficients*, which may be classified as stiffness, constraint, and energy coefficients, respectively.

In Sec. 4, we make use of two separate energy-based arguments to establish fundamental relations between the beam characteristic

---

[1]Corresponding author.

Contributed by the Mechanisms and Robotics Committee of ASME for publication in the Journal of Mechanical Design. Manuscript received October 16, 2009; final manuscript received May 16, 2010; published online August 18, 2010. Assoc. Editor: Ashitava Ghosal.

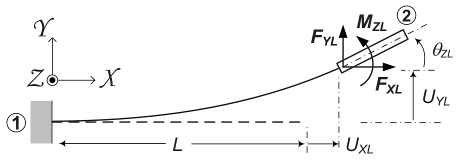

Fig. 1 Simple beam flexure

coefficients. The first is based on the PVW, and the second is based on the conservation of energy. The application of PVW at this stage also provides a consistent truncation scheme for the infinite series in the transverse load-displacement, axial geometric constraint, and strain energy expressions, as shown in Sec. 5. Since both the axial constraint and strain energy expressions exhibit a dependence on the axial load, the two expressions are combined to yield a strain energy expression free of any axial load terms. The resulting expression represents the energy formulation of the BCM. This strain energy expression for a single beam is now in a form that may be employed in conducting the load-displacement analysis of a multibeam flexure mechanism using energy methods. This is covered in Sec. 6, where the effectiveness and utility of the BCM energy formulation is highlighted using the PVW. In Sec. 7, the BCM energy formulation is further generalized to incorporate an initially slanted and/or curved beam. The paper concludes in Sec. 8 with a summary of contributions.

2 Nonlinear Strain and Strain Energy Formulation for the Beam Flexure

Figure 2 illustrates the neutral axis of a simple beam (initially straight and uniform thickness) in its undeformed (dashed line) and deformed (solid line) geometries, with respect to the indicated *X-Y-Z* coordinate axes.

$U_X(X)$ and $U_Y(X)$ represent the *X* and *Y* direction displacements of any point A_i on the beam's neutral axis. An element A_iB_i along the undeformed beam neutral axis assumes a new position and orientation A_fB_f after deformation. Therefore, the axial strain (ε_{xx}) at location *X* along the neutral axis can be stated as:

$$\begin{aligned}\varepsilon_{xx}(X,0) &= \frac{A_fB_f - A_iB_i}{A_iB_i} = [(1+U_X')^2 + U_Y'^2]^{1/2} - 1 \\ &= U_X'\left(1 - \frac{7}{16}U_X'^2 - \frac{1}{2}U_Y'^2 + \cdots\right) \\ &\quad + \frac{U_Y'^2}{2}\left(1 - \frac{5}{16}U_X'^2 - \frac{1}{4}U_Y'^2 + \cdots\right) \\ &\approx U_X' + \frac{U_Y'^2}{2}\end{aligned} \tag{1}$$

It is physically obvious that the axial displacement U_X' is much smaller than the transverse displacement U_Y'. For U_Y' less than 0.1, second and higher power terms in U_X' and U_Y' may be dropped with respect to 1 in the infinite series expansions above, with less than 1% error. Note, however, that in the final form of the strain expression, the second-power $U_Y'^2$ term has been retained with respect to the first-power U_X'—a key aspect of the nonlinear strain formulation. This second-power $U_Y'^2$ term appears because the deformed geometry (translation and rotation) of the beam neutral axis has been considered in the strain formulation; this term is comparable to the first-power U_X' even for small displacements. This expression for strain represents the true stretch of an element along the neutral axis and inherently captures the kinematics associated with the geometric constraint in the beam, i.e., beam arc length conservation.

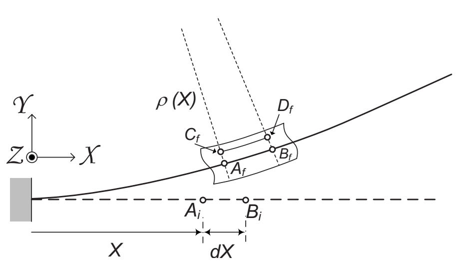

Fig. 2 Undeformed and deformed beam geometries

Next, the axial strain of an element at distance *Y* from the neutral axis, along the Y direction, may be determined by calculating the additional length change of the element C_fD_f with respect to element A_fB_f (Fig. 2). Assuming that plane sections remain plane and normal to the neutral axis after deformation (Bernoulli's assumptions), Eq. (1) may be augmented to show that

$$\begin{aligned}\varepsilon_{xx}(X,Y) &\approx U_X' + \frac{U_Y'^2}{2} - \frac{Y}{\rho(X)} = U_X' + \frac{U_Y'^2}{2} - \frac{U_Y''}{(1-U_Y'^2)^{1/2}}Y \\ &\approx U_X' + \frac{U_Y'^2}{2} - U_Y''Y\end{aligned} \tag{2}$$

where $\rho(X)$ is the curvature of the beam's neutral axis at a location that was originally at *X* before deformation [6]. Consistent with the previous approximations, the second and higher power terms in U_Y' are neglected with respect to 1 in the curvature expression in the final step above.

For a linear elastic material, the net strain energy in the beam is given by

$$V = \iiint_{Volume} \frac{E}{2}\varepsilon_{XX}^2 dA\,dX \tag{3}$$

where *E* represents the Young's modulus of the material for an *XY* plane-stress condition and the plate modulus for an *XY* plane-strain condition. Note that there is no strain energy contribution from the out-of-plane components in either of these two conditions. Furthermore, because plane sections remain plane and perpendicular to the neutral axis after deformation, the in-plane shear strain γ_{XY} is zero, and given the small *Y* direction thickness of the beam, σ_{YY} is also zero. Substituting Eq. (2) in Eq. (3) yields

$$\begin{aligned}V &= \frac{E}{2}\underbrace{\left(\int_A dA\right)}_{=A}\int_0^L \left\{U_X' + \frac{1}{2}U_Y'^2\right\}^2 dX \\ &\quad - E\underbrace{\left(\int_A Y dA\right)}_{=0}\int_0^L U_Y''\left\{U_X' + \frac{1}{2}U_Y'^2\right\}dX \\ &\quad + \frac{E}{2}\underbrace{\left(\int_A Y^2 dA\right)}_{=I_{ZZ}}\int_0^L U_Y''^2 dX \\ &= \frac{EA}{2}\int_0^L \left\{U_X' + \frac{1}{2}U_Y'^2\right\}^2 dX + \frac{EI_{ZZ}}{2}\int_0^L U_Y''^2 dX\end{aligned} \tag{4}$$

The key difference in this strain energy expression, compared with a linear formulation, is the presence of the second-power $U_Y'^2$ term in the first integral above, which inherently captures the geometric constraint of beam arc length conservation. Expression (4) is also in agreement with previous nonlinear strain energy formulations [7].

With the strain energy thus determined and the geometric boundary conditions known at the beam root ($U_X(0)=0$, $U_Y(0)$

=0, and $U_Y'(0)=0$), the PVW may be applied to the beam flexure (Fig. 1) to yield the following beam governing equations and natural boundary conditions:

- governing equations:

$$EI_{ZZ}U_Y^{iv} - \boldsymbol{F_{XL}}U_Y'' = 0 \tag{5}$$

$$U_X' + \frac{1}{2}U_Y'^2 = \frac{\boldsymbol{F_{XL}}}{EA} \tag{6}$$

- natural boundary conditions:

$$-EI_{ZZ}U_Y'''(L) + \boldsymbol{F_{XL}}U_Y'(L) = \boldsymbol{F_{YL}} \tag{7}$$

$$EI_{ZZ}U_Y''(L) - \boldsymbol{M_{ZL}} = 0 \tag{8}$$

Equation (5) provides the recognizable transverse-direction beam governing equation. This fourth order linear differential equation in U_Y is exactly the same as the one obtained in the direct formulation [1], which is to be expected because the set of assumptions made in both cases are identical. Equation (6) provides the axial-direction geometric constraint equation for the beam flexure. This reaffirms that the geometric constraint associated with the beam arc length is inherently captured in the above strain and strain energy formulations. Equation (6) may be integrated once to yield the following axial-direction relation, which is the same as the result from the direct formulation [1]:

$$U_{XL} = \frac{\boldsymbol{F_{XL}}L}{EA} - \frac{1}{2}\int_0^L U_Y'^2 dX = U_{XL}^{(e)} - \frac{1}{2}\int_0^L U_Y'^2 dX \tag{9}$$

The first term above represents the linear elastic stretching of the beam in the axial direction in response to an axial force $\boldsymbol{F_{XL}}$ and is denoted by $U_{XL}^{(e)}$. The second term captures the geometric constraint associated with beam arc length conservation. Equation (6) also corroborates the fact that its left hand side represents the true axial strain in the beam due to stretching, which remains constant throughout the beam length since the axial load and, therefore, stress, given by the right hand side of this equation, remain constant.

For a subsequent application of the PVW, the strain energy expression of Eq. (4) may be further simplified by employing Eq. (6) and invoking the definition of $U_{XL}^{(e)}$ to yield

$$V = \frac{EI_{ZZ}}{2}\int_0^L U_Y''^2 dX + \frac{AE}{2}(U_{XL}^{(e)})^2 \tag{10}$$

This clearly identifies the separate contributions to the nonlinear strain energy from beam bending and beam axial stretching. It will be seen later that the first term includes not only the bending deformation induced by the transverse loads but also that induced by the axial load.

Having thus established the consistency of the nonlinear strain energy expressions (4) and (10) with the previously reported transverse-direction beam governing equation, axial geometric constraint relation, and associated boundary conditions that led to the BCM [1], we now proceed to use these strain energy expressions as the basis for an energy-based BCM formulation.

At this stage, a normalization scheme is introduced to simplify mathematical expressions and their manipulation in the rest of this paper. All loads, displacements, position coordinates, stiffness, energy, and work terms are normalized with respect to the beam geometry and material parameters as follows:

$$\boldsymbol{f_{x1}} \triangleq \frac{\boldsymbol{F_{XL}}L^2}{EI_{ZZ}}, \quad \boldsymbol{f_{y1}} \triangleq \frac{\boldsymbol{F_{YL}}L^2}{EI_{ZZ}}, \quad \boldsymbol{m_{z1}} \triangleq \frac{\boldsymbol{M_{ZL}}L}{EI_{ZZ}},$$

$$x \triangleq \frac{X}{L}, \quad u_x(x) \triangleq \frac{U_X(X)}{L}, \quad u_y(x) \triangleq \frac{U_Y(X)}{L}, \quad u_{x1} \triangleq \frac{U_{XL}}{L},$$

$$u_{y1} \triangleq \frac{U_{YL}}{L}, \quad \theta_{z1} \triangleq \theta_{ZL} = U_Y'(X)$$

3 Load-Displacement, Geometric Constraint, and Strain Energy Expressions in Terms of End Loads and Displacements

For a simple beam, the beam governing equation (Eq. (5)) and associated geometric boundary conditions may be solved in closed form:

$$u_y(x) = c_1 e^{rx} + c_2 e^{-rx} + c_3 x + c_4 \quad \text{where } \boldsymbol{r}^2 \triangleq \boldsymbol{f_{x1}}$$

$$c_1 = \frac{\boldsymbol{r}(e^{-\boldsymbol{r}}-1)u_{y1} + (e^{-\boldsymbol{r}}+\boldsymbol{r}-1)\theta_{z1}}{\boldsymbol{r}[\boldsymbol{r}(e^{\boldsymbol{r}}-e^{-\boldsymbol{r}}) - 2(e^{\boldsymbol{r}}+e^{-\boldsymbol{r}})+4]},$$

$$c_2 = \frac{\boldsymbol{r}(e^{\boldsymbol{r}}-1)u_{y1} - (e^{\boldsymbol{r}}-\boldsymbol{r}-1)\theta_{z1}}{\boldsymbol{r}[\boldsymbol{r}(e^{\boldsymbol{r}}-e^{-\boldsymbol{r}}) - 2(e^{\boldsymbol{r}}+e^{-\boldsymbol{r}})+4]} \tag{11}$$

$$c_3 = \boldsymbol{r}(c_2 - c_1), \quad c_4 = -c_1 - c_2$$

The intermediary variable $\boldsymbol{r}(\triangleq \boldsymbol{f_{x1}}^{1/2})$ is introduced temporarily for mathematical convenience. The application of natural boundary conditions (7) and (8) in the above expression yields the following transverse-direction end load-displacement relations:

$$\begin{Bmatrix} \boldsymbol{f_{y1}} \\ \boldsymbol{m_{z1}} \end{Bmatrix} = \begin{bmatrix} \dfrac{\boldsymbol{r}^3 \sinh \boldsymbol{r}}{\boldsymbol{r}\sinh \boldsymbol{r} - 2\cosh \boldsymbol{r} + 2} & -\dfrac{\boldsymbol{r}^2(\cosh \boldsymbol{r} - 1)}{\boldsymbol{r}\sinh \boldsymbol{r} - 2\cosh \boldsymbol{r} + 2} \\ -\dfrac{\boldsymbol{r}^2(\cosh \boldsymbol{r} - 1)}{\boldsymbol{r}\sinh \boldsymbol{r} - 2\cosh \boldsymbol{r} + 2} & \dfrac{\boldsymbol{r}^2\cosh \boldsymbol{r} - \boldsymbol{r}\sinh \boldsymbol{r}}{\boldsymbol{r}\sinh \boldsymbol{r} - 2\cosh \boldsymbol{r} + 2} \end{bmatrix} \times \begin{Bmatrix} u_{x1} \\ \theta_{z1} \end{Bmatrix} \tag{12}$$

In this nonlinear formulation, the stiffness terms are no longer simply elastic terms as in the purely linear case but are instead functions of the axial load $\boldsymbol{f_{x1}}$. These transcendental expressions may be expanded in $\boldsymbol{f_{x1}}$ to yield the following infinite series:

$$\begin{Bmatrix} \boldsymbol{f_{y1}} \\ \boldsymbol{m_{z1}} \end{Bmatrix} = \begin{bmatrix} 12 & -6 \\ -6 & 4 \end{bmatrix} \begin{Bmatrix} u_{x1} \\ \theta_{z1} \end{Bmatrix} + \boldsymbol{f_{x1}} \begin{bmatrix} \dfrac{6}{5} & -\dfrac{1}{10} \\ -\dfrac{1}{10} & \dfrac{2}{15} \end{bmatrix} \begin{Bmatrix} u_{x1} \\ \theta_{z1} \end{Bmatrix} + \boldsymbol{f_{x1}^2} \begin{bmatrix} -\dfrac{1}{700} & \dfrac{1}{1400} \\ \dfrac{1}{1400} & -\dfrac{11}{6300} \end{bmatrix} \begin{Bmatrix} u_{x1} \\ \theta_{z1} \end{Bmatrix} + \boldsymbol{f_{x1}^3} \begin{bmatrix} \dfrac{1}{63{,}000} & -\dfrac{1}{126{,}000} \\ -\dfrac{1}{126{,}000} & \dfrac{1}{27{,}000} \end{bmatrix} \begin{Bmatrix} u_{x1} \\ \theta_{z1} \end{Bmatrix} + \cdots \tag{13}$$

In the BCM, the first matrix in the above series captures the elastic stiffness and the second matrix captures load stiffening, which quantifies the change in DoF direction effective stiffness in the presence of a DoC load [2]. Higher power terms are found to have negligible contributions (<1%) for $\boldsymbol{f_{x1}}$ less than ±5.0, which is a practically relevant range in flexure mechanisms.

Next, the solution given by Eq. (11) may be substituted in Eq. (9) to obtain the axial-direction geometric constraint equation in terms of end loads and displacements:

$$u_{x1} = u_{x1}^{(e)} + \begin{Bmatrix} u_{y1} & \theta_{z1} \end{Bmatrix} \begin{bmatrix} g_{11} & g_{12} \\ g_{21} & g_{22} \end{bmatrix} \begin{Bmatrix} u_{y1} \\ \theta_{z1} \end{Bmatrix} \tag{14}$$

where

$$g_{11} = -\frac{\boldsymbol{r}^2(\cosh \boldsymbol{r}+2)(\cosh \boldsymbol{r}-1) - 3\boldsymbol{r}\sinh \boldsymbol{r}(\cosh \boldsymbol{r}-1)}{2(\boldsymbol{r}\sinh \boldsymbol{r} - 2\cosh \boldsymbol{r}+2)^2}$$

$$g_{12} = g_{21} = \frac{\boldsymbol{r}^2(\cosh \boldsymbol{r}-1) + \boldsymbol{r}\sinh \boldsymbol{r}(\cosh \boldsymbol{r}-1) - 4(\cosh \boldsymbol{r}-1)^2}{4(\boldsymbol{r}\sinh \boldsymbol{r} - 2\cosh \boldsymbol{r}+2)^2} \tag{15}$$

$$g_{22} = \frac{\boldsymbol{r}^3 - \boldsymbol{r}^2\sinh \boldsymbol{r}(\cosh \boldsymbol{r}+2) + 2\boldsymbol{r}(2\cosh \boldsymbol{r}+1)(\cosh \boldsymbol{r}-1) - 2\sinh \boldsymbol{r}(\cosh \boldsymbol{r}-1)}{4\boldsymbol{r}(\boldsymbol{r}\sinh \boldsymbol{r} - 2\cosh \boldsymbol{r}+2)^2}$$

$$u_{x1}^{(e)} = \frac{\boldsymbol{f_{x1}}}{k_{33}} \quad \text{and} \quad k_{33} = \frac{12}{t^2}$$

This axial-direction relation for the DoC end displacement u_{x1} in terms of DoF end displacements, u_{y1} and θ_{z1}, and DoC end load $\boldsymbol{f_{x1}}$ is as expected [2]. Since this expression arises from the purely geometric constraint of the constant beam arc length, the presence of the axial load $\boldsymbol{f_{x1}}$ in the constraint terms g is initially surprising. While uncommon in mechanics, this does highlight the unique attributes of distributed compliance mechanisms and will be shown to be responsible for the elastokinematic effect in the BCM. The transcendental expressions for the constraint terms may be expanded in terms of $\boldsymbol{f_{x1}}$ to yield the following infinite series:

$$\begin{aligned} u_{x1} = u_{x1}^{(e)} &+ \{u_{y1} \quad \theta_{z1}\} \begin{bmatrix} -\frac{3}{5} & \frac{1}{20} \\ \frac{1}{20} & -\frac{1}{15} \end{bmatrix} \begin{Bmatrix} u_{y1} \\ \theta_{z1} \end{Bmatrix} \\ &+ \boldsymbol{f_{x1}}\{u_{y1} \quad \theta_{z1}\} \begin{bmatrix} \frac{1}{700} & -\frac{1}{1400} \\ -\frac{1}{1400} & \frac{11}{6300} \end{bmatrix} \begin{Bmatrix} u_{x1} \\ \theta_{z1} \end{Bmatrix} \\ &+ \boldsymbol{f_{x1}^2}\{u_{y1} \quad \theta_{z1}\} \begin{bmatrix} -\frac{1}{42{,}000} & \frac{1}{84{,}000} \\ \frac{1}{84{,}000} & -\frac{1}{18{,}000} \end{bmatrix} \begin{Bmatrix} u_{x1} \\ \theta_{z1} \end{Bmatrix} + \cdots \end{aligned} \tag{16}$$

The first term in this series expansion (zeroth power of $\boldsymbol{f_{x1}}$) indicates a component that is explicitly and exclusively dependent on the transverse end displacements u_{y1} and θ_{z1} and is independent of any loads. Therefore, this term is referred to as the kinematic component of the axial displacement and is denoted by $u_{x1}^{(k)}$. The next term, although small compared with the first term, is comparable to the purely elastic term $u_{x1}^{(e)}$ and therefore cannot be ignored. Even though this term arises from the geometric constraint of beam arc length conservation, it does have a linear dependence on $\boldsymbol{f_{x1}}$ and therefore contributes to the compliance along the DoC direction. This term, referred to as the elastokinematic component in the BCM and denoted by $u_{x1}^{(e-k)}$, is unusual and a unique outcome of distributed compliance. The consideration of the beam in its deformed configuration in formulating the nonlinear strain and strain energy in Sec. 3 ensures that the contribution of the axial load $\boldsymbol{f_{x1}}$ to the bending moments at any given beam cross section is appropriately captured. Because of the beam's distributed compliance, this additional bending moment causes a change in its deformation, which produces the elastokinematic displacement $u_{x1}^{(e-k)}$ along the DoC direction, even as the DoF displacements u_{y1} and θ_{z1} remain constant.

Second and higher power $\boldsymbol{f_{x1}}$ terms in the above expression have a negligible contribution ($<1\%$) in the load and displacement ranges of interest.

Next, we proceed to determine the strain energy in terms of end displacements. Note that it would be incorrect to simply employ the stiffness expression (12) determined above to find the strain energy. The stiffness given by this expression is the effective stiffness in the sense that it also captures load stiffening, which is a consequence of the geometry and not deformation, and therefore does not contribute to the strain energy. The strain energy may be accurately determined by substituting the beam deformation expression (11) in Eq. (10),

$$v = \frac{1}{2}\{u_{y1} \quad \theta_{z1}\} \begin{bmatrix} v_{11} & v_{12} \\ v_{21} & v_{22} \end{bmatrix} \begin{Bmatrix} u_{y1} \\ \theta_{z1} \end{Bmatrix} + \frac{1}{2}k_{33}(u_{x1}^{(e)})^2$$

where

$$v_{11} = \frac{\boldsymbol{r}^3(\sinh \boldsymbol{r} - \boldsymbol{r})(\cosh \boldsymbol{r}-1)}{(\boldsymbol{r}\sinh \boldsymbol{r} - 2\cosh \boldsymbol{r}+2)^2}$$

$$v_{12} = v_{21} = -\frac{1}{2}\frac{\boldsymbol{r}^3(\sinh \boldsymbol{r} - \boldsymbol{r})(\cosh \boldsymbol{r}-1)}{(\boldsymbol{r}\sinh \boldsymbol{r} - 2\cosh \boldsymbol{r}+2)^2} \tag{17}$$

$$v_{22} = \frac{1}{2}\frac{(\boldsymbol{r}^3\sinh \boldsymbol{r} - 2\boldsymbol{r}^2\cosh \boldsymbol{r} + 2\boldsymbol{r}\sinh \boldsymbol{r})(\cosh \boldsymbol{r}-1) - \boldsymbol{r}^3(\sinh \boldsymbol{r} - \boldsymbol{r})}{(\boldsymbol{r}\sinh \boldsymbol{r} - 2\cosh \boldsymbol{r}+2)^2}$$

The first term above represents energy due to beam bending, while the second term represents energy due to the axial stretching of the beam arc length. What is unusual is that the bending strain energy is not simply dependent on the transverse end displacements u_{y1} and θ_{z1}, but also on the axial load ($\boldsymbol{f_{x1}} \triangleq \boldsymbol{r^2}$). This is simply a consequence of the fact that even when the transverse end displacements are held fixed, the axial load can produce additional bending moment along the beam shape, which results in an additional bending deformation of the beam, thus contributing an additional component of energy. This is the manifestation of the elastokinematic effect in the strain energy domain. The transcendental terms in Eq. (17) may be expanded in $\boldsymbol{f_{x1}}$ to yield the following infinite series:

$$v = \frac{1}{2}k_{33}(u_{x1}^{(e)})^2 + \frac{1}{2}\{u_{y1} \quad \theta_{z1}\}\begin{bmatrix} 12 & -6 \\ -6 & 4 \end{bmatrix}\begin{Bmatrix} u_{y1} \\ \theta_{z1} \end{Bmatrix} + \frac{1}{2}\boldsymbol{f}_{\boldsymbol{x1}}^2\{u_{y1} \quad \theta_{z1}\}\begin{bmatrix} \frac{1}{700} & -\frac{1}{1400} \\ -\frac{1}{1400} & \frac{11}{6300} \end{bmatrix}\begin{Bmatrix} u_{y1} \\ \theta_{z1} \end{Bmatrix} + \frac{1}{2}\boldsymbol{f}_{\boldsymbol{x1}}^3\{u_{y1} \quad \theta_{z1}\}\begin{bmatrix} -\frac{1}{31,500} & \frac{1}{63,000} \\ \frac{1}{63,000} & -\frac{1}{13,500} \end{bmatrix}\begin{Bmatrix} u_{y1} \\ \theta_{z1} \end{Bmatrix} + \cdots \tag{18}$$

For an axial load range of practical interest ($\boldsymbol{f}_{\boldsymbol{x1}}$ less than ± 5.0), only the first load term, which is quadratic in $\boldsymbol{f}_{\boldsymbol{x1}}$, is significant, and the higher power terms may be neglected. Moreover, there appears to be some similarity between the stiffness and energy coefficients of the corresponding powers of $\boldsymbol{f}_{\boldsymbol{x1}}$ in Eqs. (13) and (18). In fact, the zeroth-power coefficients are the same, showing that the biggest portion of the strain energy comes from the elastic stiffness in the transverse direction. Interestingly, there is no first-power term in the energy expression corresponding to the first-power term in the stiffness expression, which is associated with the load-stiffening effect. This agrees with a physical understanding of the system—since the load-stiffening effect is a consequence of geometry and not deformation, it should not contribute any strain energy. Subsequent stiffness and energy coefficients of corresponding powers of $\boldsymbol{f}_{\boldsymbol{x1}}$ show some similarity but are not identical. Furthermore, there also appears to be some similarity between the stiffness coefficients of a certain power of $\boldsymbol{f}_{\boldsymbol{x1}}$ in Eq. (16) and the constraint coefficients associated with one lower power of $\boldsymbol{f}_{\boldsymbol{x1}}$ in Eq. (18). Thus, the natural question that arises is whether there is some underlying relationship between these stiffness, constraint, and energy coefficients of the various powers of $\boldsymbol{f}_{\boldsymbol{x1}}$ in Eqs. (13), (16), and (18), respectively, or if this similarity is merely a coincidence.

Another question that remains to be answered is where to truncate the infinite series associated with the stiffness, constraint, and energy expressions for the purpose of obtaining an accurate yet compact beam constraint model. In the explicit formulation, we dealt with only two relations—the transverse-direction load-displacement relation and the axial-direction geometric constraint relation. Both relations were truncated to keep only the first-power term in $\boldsymbol{f}_{\boldsymbol{x1}}$, and it was noted that this led to errors less than 1% over an axial load range of ± 5 and transverse displacement range of ± 0.1 [1,2]. Now, we have a third relation that captures the strain energy of the beam flexure. It is not clear if this third expression, or even the first two, can be truncated independent of each other or if a certain scheme has to be followed so that the truncated expressions are "consistent" with respect to each other. The similarity between the coefficients noted earlier seems to indicate that there should be a consistent truncation scheme that at least ensures that the PVW is valid even for the truncated expressions.

However, before taking up the above two questions in Sec. 4, we first proceed to show that the format of Eqs. (13), (16), and (18) accommodates any general beam shape and not just a uniform-thickness beam. The beam deformation, end loading, and end displacement representations for the variable cross-section beam remain the same as in Fig. 1. The modeling assumptions are also the same as earlier, except that the beam thickness is now a function of X: $T(X) = T_0\xi(X)$, where T_0 is the nominal beam thickness at the beam root and $\xi(X)$ represents the beam shape variation. Thus, the second moment of area becomes $I_{ZZ}(X) = I_{ZZ0}\xi^3(X)$. The normalization scheme remains the same as earlier, with the exception that I_{ZZ0} is now used in place of I_{ZZ}. Following a PVW procedure analogous to the one outlined in Sec. 2, one may derive the following normalized governing equations and natural boundary conditions for this case:

- governing equations:

$$(\xi^3(x)u_y''(x))'' - \boldsymbol{f}_{\boldsymbol{x1}}u_y''(x) = 0 \tag{19}$$

$$u_x'(x) + \frac{1}{2}u_y'^2(x) = \boldsymbol{f}_{\boldsymbol{x1}}\frac{t_0^2}{12\xi(x)} \tag{20}$$

- natural boundary conditions:

$$-\{\xi^3(1)u_y''(1)\}' + \boldsymbol{f}_{\boldsymbol{x1}}u_y'(1) = \boldsymbol{f}_{\boldsymbol{y1}} \tag{21}$$

$$\xi^3(1)u_y''(1) - \boldsymbol{m}_{\boldsymbol{z1}} = 0 \tag{22}$$

Given the arbitrariness of $\xi(x)$, a closed-form solution to this ordinary differential equation with variable coefficients (Eq. (19)) is no longer possible. Nevertheless, the equation and boundary conditions remain linear in the transverse loads ($\boldsymbol{f}_{\boldsymbol{y1}}$ and $\boldsymbol{m}_{\boldsymbol{z1}}$) and transverse displacements ($u_y(x)$ and its derivatives). This implies that the resulting relation between the transverse end loads and end displacement also has to be linear, of the form

$$\begin{Bmatrix} \boldsymbol{f}_{\boldsymbol{y1}} \\ \boldsymbol{m}_{\boldsymbol{z1}} \end{Bmatrix} = \begin{bmatrix} k_{11}(\boldsymbol{f}_{\boldsymbol{x1}};\xi(x)) & k_{12}(\boldsymbol{f}_{\boldsymbol{x1}};\xi(x)) \\ k_{21}(\boldsymbol{f}_{\boldsymbol{x1}};\xi(x)) & k_{22}(\boldsymbol{f}_{\boldsymbol{x1}};\xi(x)) \end{bmatrix}\begin{Bmatrix} u_{y1} \\ \theta_{z1} \end{Bmatrix} \tag{23}$$

The effective stiffness terms (k's) will now be some functions of the axial load $\boldsymbol{f}_{\boldsymbol{x1}}$, dictated by the beam shape $\xi(x)$, and might be difficult or impossible to determine in closed form. Nevertheless, these functions may certainly be expanded as a generic infinite series in $\boldsymbol{f}_{\boldsymbol{x1}}$,

$$\begin{Bmatrix} \boldsymbol{f}_{\boldsymbol{y1}} \\ \boldsymbol{m}_{\boldsymbol{z1}} \end{Bmatrix} = \begin{bmatrix} k_{11}^{(0)} & k_{12}^{(0)} \\ k_{12}^{(0)} & k_{22}^{(0)} \end{bmatrix}\begin{Bmatrix} u_{y1} \\ \theta_{z1} \end{Bmatrix} + \boldsymbol{f}_{\boldsymbol{x1}}\begin{bmatrix} k_{11}^{(1)} & k_{12}^{(1)} \\ k_{12}^{(1)} & k_{22}^{(1)} \end{bmatrix}\begin{Bmatrix} u_{y1} \\ \theta_{z1} \end{Bmatrix} + \boldsymbol{f}_{\boldsymbol{x1}}^2\begin{bmatrix} k_{11}^{(2)} & k_{12}^{(2)} \\ k_{12}^{(2)} & k_{22}^{(2)} \end{bmatrix}\begin{Bmatrix} u_{y1} \\ \theta_{z1} \end{Bmatrix} + \cdots = \sum_{n=0}^{\infty}\boldsymbol{f}_{\boldsymbol{x1}}^n\begin{bmatrix} k_{11}^{(n)} & k_{12}^{(n)} \\ k_{12}^{(n)} & k_{22}^{(n)} \end{bmatrix}\begin{Bmatrix} u_{y1} \\ \theta_{z1} \end{Bmatrix} \tag{24}$$

Similarly, it may be shown that irrespective of the beam shape, the constraint equation may be stated and expanded as

$$u_{x1} = u_{x1}^{(e)} + \{u_{y1} \quad \theta_{z1}\}\begin{bmatrix} g_{11}(\boldsymbol{f}_{\boldsymbol{x1}};\xi(x)) & g_{12}(\boldsymbol{f}_{\boldsymbol{x1}};\xi(x)) \\ g_{21}(\boldsymbol{f}_{\boldsymbol{x1}};\xi(x)) & g_{22}(\boldsymbol{f}_{\boldsymbol{x1}};\xi(x)) \end{bmatrix}\begin{Bmatrix} u_{y1} \\ \theta_{z1} \end{Bmatrix}$$
$$= \boldsymbol{f}_{\boldsymbol{x1}}\frac{t_0^2}{12}\left\{\int_0^1 \frac{dx}{\xi(x)}\right\} + \{u_{y1} \quad \theta_{z1}\}\begin{bmatrix} g_{11}^{(0)} & g_{12}^{(0)} \\ g_{12}^{(0)} & g_{22}^{(0)} \end{bmatrix}\begin{Bmatrix} u_{y1} \\ \theta_{z1} \end{Bmatrix} + \boldsymbol{f}_{\boldsymbol{x1}}\{u_{y1} \quad \theta_{z1}\}\begin{bmatrix} g_{11}^{(1)} & g_{12}^{(1)} \\ g_{12}^{(1)} & g_{22}^{(1)} \end{bmatrix}\begin{Bmatrix} u_{x1} \\ \theta_{z1} \end{Bmatrix} + \boldsymbol{f}_{\boldsymbol{x1}}^2\{u_{y1} \quad \theta_{z1}\}\begin{bmatrix} g_{11}^{(2)} & g_{12}^{(2)} \\ g_{12}^{(2)} & g_{22}^{(2)} \end{bmatrix}\begin{Bmatrix} u_{x1} \\ \theta_{z1} \end{Bmatrix} + \cdots$$
$$= \frac{\boldsymbol{f}_{\boldsymbol{x1}}}{k_{33}} + \sum_{n=0}^{\infty}\boldsymbol{f}_{\boldsymbol{x1}}^n\{u_{y1} \quad \theta_{z1}\}\begin{bmatrix} g_{11}^{(n)} & g_{12}^{(n)} \\ g_{12}^{(n)} & g_{22}^{(n)} \end{bmatrix}\begin{Bmatrix} u_{y1} \\ \theta_{z1} \end{Bmatrix} \tag{25}$$

Along the same lines, the strain energy for a variable cross-section beam may be shown to be quadratic in the transverse displacements, u_{y1} and θ_{z1}, and some unknown function of the axial load $\boldsymbol{f}_{\boldsymbol{x1}}$. This expression may be expanded as follows:

$$v = \frac{1}{2}\{u_{y1} \quad \theta_{z1}\}\begin{bmatrix} v_{11}(\boldsymbol{f_{x1}};\xi(x)) & v_{12}(\boldsymbol{f_{x1}};\xi(x)) \\ v_{21}(\boldsymbol{f_{x1}};\xi(x)) & v_{22}(\boldsymbol{f_{x1}};\xi(x)) \end{bmatrix}\begin{Bmatrix} u_{y1} \\ \theta_{z1} \end{Bmatrix} + \frac{1}{2}k_{33}u_{x1}^{(e)^2}$$
$$= \frac{1}{2}\{u_{y1} \quad \theta_{z1}\}\begin{bmatrix} v_{11}^{(0)} & v_{12}^{(0)} \\ v_{12}^{(0)} & v_{22}^{(0)} \end{bmatrix}\begin{Bmatrix} u_{y1} \\ \theta_{z1} \end{Bmatrix} + \frac{1}{2}\boldsymbol{f_{x1}}\{u_{y1} \quad \theta_{z1}\}\begin{bmatrix} v_{11}^{(1)} & v_{12}^{(1)} \\ v_{12}^{(1)} & v_{22}^{(1)} \end{bmatrix}$$
$$\times\begin{Bmatrix} u_{y1} \\ \theta_{z1} \end{Bmatrix} + \frac{1}{2}\boldsymbol{f_{x1}^2}\{u_{y1} \quad \theta_{z1}\}\begin{bmatrix} v_{11}^{(2)} & v_{12}^{(2)} \\ v_{12}^{(2)} & v_{22}^{(2)} \end{bmatrix}\begin{Bmatrix} u_{x1} \\ \theta_{z1} \end{Bmatrix} + \cdots$$
$$+ \frac{1}{2}k_{33}u_{x1}^{(e)^2} = \frac{1}{2}\sum_{n=0}^{\infty}\boldsymbol{f_{x1}^n}\{u_{y1} \quad \theta_{z1}\}\begin{bmatrix} v_{11}^{(n)} & v_{12}^{(n)} \\ v_{12}^{(n)} & v_{22}^{(n)} \end{bmatrix}\begin{Bmatrix} u_{y1} \\ \theta_{z1} \end{Bmatrix} + \frac{1}{2}k_{33}u_{x1}^{(e)^2} \quad (26)$$

4 Fundamental Relations Between Beam Characteristic Coefficients

Having derived the generic expressions (24)–(26) for the transverse stiffness, axial constraint, and strain energy for an initially straight beam with any generalized shape, the next step is to determine if there are any fundamental relations between these three expressions and their associated beam characteristic coefficients. To do so, we employ the PVW once again. These three expressions, explicit in terms of the end loads and end displacements, have been derived from the implicit expressions (5), (6), and (10), respectively. Since these implicit expressions were shown to be consistent with each other via PVW in Sec. 2, the resulting explicit expressions should also be consistent with regard to PVW.

Thus, a variation in the strain energy, given by Eq. (26), keeping the external loads constant, in response to virtual displacements δu_{x1}, δu_{y1}, and $\delta\theta_{z1}$ that satisfy the geometric constraint condition (25), can be equated to the virtual work done by the external forces over these virtual displacements. This implies that

$$\delta v = \boldsymbol{f_{x1}}\delta u_{x1} + \boldsymbol{f_{y1}}\delta u_{y1} + \boldsymbol{m_{z1}}\delta\theta_{z1}$$
$$\Rightarrow \sum_{n=0}^{\infty}\boldsymbol{f_{x1}^n}\{\delta u_{y1} \quad \delta\theta_{z1}\}\begin{bmatrix} v_{11}^{(n)} & v_{12}^{(n)} \\ v_{12}^{(n)} & v_{22}^{(n)} \end{bmatrix}\begin{Bmatrix} u_{y1} \\ \theta_{z1} \end{Bmatrix} + k_{33}u_{x1}^{(e)}\delta u_{x1}^{(e)}$$
$$= 2\sum_{n=0}^{\infty}\boldsymbol{f_{x1}^{n+1}}\{\delta u_{y1} \quad \delta\theta_{z1}\}\begin{bmatrix} g_{11}^{(n)} & g_{12}^{(n)} \\ g_{12}^{(n)} & g_{22}^{(n)} \end{bmatrix}\begin{Bmatrix} u_{y1} \\ \theta_{z1} \end{Bmatrix}$$
$$+ \boldsymbol{f_{x1}}\delta u_{x1}^{(e)} + \boldsymbol{f_{y1}}\delta u_{y1} + \boldsymbol{m_{z1}}\delta\theta_{z1} \quad (27)$$

Since the virtual displacements δu_{x1}, δu_{y1}, and $\delta\theta_{z1}$ are arbitrary, their respective coefficients may be set to zero. This leads to the following end load-displacement relations:

$$\boldsymbol{f_{x1}} = k_{33}u_{x1}^{(e)} \quad (28)$$

$$\begin{Bmatrix} \boldsymbol{f_{y1}} \\ \boldsymbol{m_{z1}} \end{Bmatrix} = \begin{bmatrix} v_{11}^{(0)} & v_{12}^{(0)} \\ v_{12}^{(0)} & v_{22}^{(0)} \end{bmatrix}\begin{Bmatrix} u_{y1} \\ \theta_{z1} \end{Bmatrix} + \left(\sum_{n=1}^{\infty}\boldsymbol{f_{x1}^n}\begin{bmatrix} v_{11}^{(n)} - 2g_{11}^{(n-1)} & v_{12}^{(n)} - 2g_{12}^{(n-1)} \\ v_{12}^{(n)} - 2g_{12}^{(n-1)} & v_{22}^{(n)} - 2g_{22}^{(n-1)} \end{bmatrix}\right)\begin{Bmatrix} u_{y1} \\ \theta_{z1} \end{Bmatrix} \quad (29)$$

Equation (28) is an expected result and provides no new information. However, a comparison between Eqs. (29) and (24), both of which should be identical, given the above-mentioned consistency in the energy formulation, reveals a fundamental relation between the stiffness, constraint, and energy coefficients,

$$k_{\beta\lambda}^{(0)} = v_{\beta\lambda}^{(0)}$$
$$k_{\beta\lambda}^{(n)} = v_{\beta\lambda}^{(n)} - 2g_{\beta\lambda}^{(n-1)}, \quad \forall\, n = 1, \ldots, \infty \quad (30)$$

where β and λ both take indicial values of 1 and 2. This explains some of the similarities observed at the end of Sec. 3. The above relations may be readily verified for the case of a simple beam using the known results (Eqs. (13), (16), and (18)); however, it should be noted that these are valid for any general beam shape, as proven above.

A second argument based on the conservation of energy provides yet another fundamental relation between the beam characteristic coefficients. Since a given set of end loads ($\boldsymbol{f_{x1}}$, $\boldsymbol{f_{y1}}$, and $\boldsymbol{m_{z1}}$) produces a unique set of end displacements (u_{x1}, u_{y1}, and θ_{z1}), the resulting strain energy stored in the deformed beam is also unique, as given by Eq. (26). This strain energy remains the same irrespective of the order in which the loading is carried out. Therefore, we consider a case where the loading is performed in two steps: (1) End loads $\boldsymbol{f_{y1}}$ and $\boldsymbol{m_{z1}}$ are applied to produce some end displacements $\bar{u}_{x1}$, u_{y1}, and θ_{z1}. (2) While holding the end displacements u_{y1} and θ_{z1} fixed, end load $\boldsymbol{f_{x1}}$ is applied to change the axial displacement from $\bar{u}_{x1}$ to u_{x1}.

The sum of energy added to the beam in these two steps should be equal to the final strain energy given by Eq. (26). Energy stored in step 1 is simply obtained by setting $\boldsymbol{f_{x1}}=0$ in Eq. (26),

$$v_1 = \frac{1}{2}\{u_{y1} \quad \theta_{z1}\}\begin{bmatrix} v_{11}^{(0)} & v_{12}^{(0)} \\ v_{12}^{(0)} & v_{22}^{(0)} \end{bmatrix}\begin{Bmatrix} u_{y1} \\ \theta_{z1} \end{Bmatrix} \quad (31)$$

The axial displacement at the end of step 1 is given by setting $\boldsymbol{f_{x1}}=0$ in Eq. (25),

$$\bar{u}_{x1} = \{u_{y1} \quad \theta_{z1}\}\begin{bmatrix} g_{11}^{(0)} & g_{12}^{(0)} \\ g_{12}^{(0)} & g_{22}^{(0)} \end{bmatrix}\begin{Bmatrix} u_{y1} \\ \theta_{z1} \end{Bmatrix} \quad (32)$$

Next, assuming a conservative system, the energy added to the beam in step 2 may simply be determined by calculating the work done on the system when force $\boldsymbol{f_{x1}}$ causes the beam end to move from $\bar{u}_{x1}$ to u_{x1} in the axial direction. An integral needs to be carried out since the relation between $\boldsymbol{f_{x1}}$ and u_{x1} is nonlinear. However, since inverting Eq. (25), which provides displacement in terms of force, is not trivial, determining the work done in this fashion is difficult if not impossible. Therefore, instead we choose to determine the complementary work, which is readily derived from Eq. (25):

$$v_2^*(\boldsymbol{f_{x1}}) = w_2^*(\boldsymbol{f_{x1}}) = \int_0^{\boldsymbol{f_{x1}}}(u_{x1} - \bar{u}_{x1}) \cdot d\boldsymbol{f_{x1}} \quad (33)$$

This result is then used to calculate the strain energy stored in the beam during step 2 as follows:

$$v_2(u_{x1}) = (u_{x1} - \bar{u}_{x1}) \cdot \boldsymbol{f_{x1}} - v_2^*(\boldsymbol{f_{x1}}) \quad (34)$$

Substituting Eqs. (25) and (32) first in Eq. (33) and then all these three in Eq. (34) yields

$$v_2 = \boldsymbol{f_{x1}}\frac{\boldsymbol{f_{x1}}}{k_{33}} + \sum_{n=1}^{\infty}\boldsymbol{f_{x1}^{n+1}}\{u_{y1} \quad \theta_{z1}\}\begin{bmatrix} g_{11}^{(n)} & g_{12}^{(n)} \\ g_{12}^{(n)} & g_{22}^{(n)} \end{bmatrix}\begin{Bmatrix} u_{y1} \\ \theta_{z1} \end{Bmatrix} - \frac{\boldsymbol{f_{x1}^2}}{2k_{33}}$$
$$- \sum_{n=1}^{\infty}\frac{1}{n+1}\boldsymbol{f_{x1}^{n+1}}\{u_{y1} \quad \theta_{z1}\}\begin{bmatrix} g_{11}^{(n)} & g_{12}^{(n)} \\ g_{12}^{(n)} & g_{22}^{(n)} \end{bmatrix}\begin{Bmatrix} u_{y1} \\ \theta_{z1} \end{Bmatrix}$$
$$= \frac{\boldsymbol{f_{x1}^2}}{2k_{33}} + \sum_{n=1}^{\infty}\left(\frac{n}{n+1}\boldsymbol{f_{x1}^{n+1}}\{u_{y1} \quad \theta_{z1}\}\begin{bmatrix} g_{11}^{(n)} & g_{12}^{(n)} \\ g_{12}^{(n)} & g_{22}^{(n)} \end{bmatrix}\begin{Bmatrix} u_{y1} \\ \theta_{z1} \end{Bmatrix}\right)$$
$$= \frac{\boldsymbol{f_{x1}^2}}{2k_{33}} + \sum_{n=1}^{\infty}\left(\frac{n-1}{n}\boldsymbol{f_{x1}^{n}}\{u_{y1} \quad \theta_{z1}\}\begin{bmatrix} g_{11}^{(n-1)} & g_{12}^{(n-1)} \\ g_{12}^{(n-1)} & g_{22}^{(n-1)} \end{bmatrix}\begin{Bmatrix} u_{y1} \\ \theta_{z1} \end{Bmatrix}\right) \quad (35)$$

Since $v=v_1+v_2$, Eqs. (26), (31), and (35) imply that there is another fundamental relation between the energy and constraint coefficients, given by

$$v_{\beta\lambda}^{(n)} = 2\left(\frac{n-1}{n}\right)g_{\beta\lambda}^{(n-1)}, \quad \forall\, n = 1, \ldots, \infty \quad (36)$$

Expressions (30) and (36) may be further manipulated to yield the following relations between stiffness and constraint coefficients, and energy and stiffness coefficients:

$$k_{\beta\lambda}^{(n)} = -\frac{2}{n} g_{\beta\lambda}^{(n-1)}, \quad \forall\, n = 1, \ldots, \infty \tag{37}$$

$$\begin{aligned} v_{\beta\lambda}^{(0)} &= k_{\beta\lambda}^{(0)} \\ v_{\beta\lambda}^{(n)} &= -(n-1) k_{\beta\lambda}^{(n)}, \quad \forall\, n = 1, \ldots, \infty \end{aligned} \tag{38}$$

Together, Eqs. (36)–(38) present the far-reaching conclusion that the stiffness, constraint, and energy expressions are all inter-related; any one can be expressed in terms of any of the other two. These relations may be readily verified for the known case of a simple beam via Eqs. (13), (16), and (18) but are true for any general beam shape, as proven above. Moreover, these relations offer considerable insight into the nature of the nonlinear results for variable cross-section beam flexures. Some specific observations are noted below:

1. Equation (38) indicates that no matter what the beam shape is, $v_{\beta\lambda}^{(1)}$ is always zero. This simply implies that while all other stiffness coefficients contribute to the strain energy, the stiffness coefficient associated with the first power of $\boldsymbol{f_{x1}}$, which represents a load stiffening, does not.
2. Equation (37) shows that $k_{\beta\lambda}^{(1)} = -2 g_{\beta\lambda}^{(0)}$, irrespective of the beam shape. This indicates that the load-stiffening effect seen in the transverse-direction load-displacement relation and the kinematic component seen in the axial-direction geometric constraint relation are inherently related. In hindsight, this is physically reasonable because both these effects arise from the consideration of the beam in a deformed configuration.
3. The above relations also highlight the fact that the transverse load-displacement expression (24), the axial geometric constraint expression (25), and the strain energy expression (26) for a generalized beam are not entirely independent. The geometric constraint expression captures all the beam characteristic coefficients, except for the elastic stiffness $k_{\beta\lambda}^{(0)}$. The strain energy, on the other hand, captures all the beam characteristic coefficients except for load stiffening and kinematic ones. However, the transverse-direction load-displacement relation is the most complete of the three in that it captures all the beam characteristic coefficients. This is reasonable because as per the PVW, both the strain energy and geometric constraint relations are used in deriving the transverse load-displacement relation.

This last observation leads to an important practical advantage. It implies that in the derivation of the nonlinear transverse stiffness, constraint, and energy relations for a beam, which ultimately lead to the BCM, it is no longer necessary to determine all three individually. In fact, solving for the constraint and energy relations individually is mathematically more tedious because of the integration steps and the quadratic terms in u_{y1} and θ_{z1} involved. Instead, one may simply derive the transverse load-displacement relation and determine the constraint and energy relations indirectly using Eqs. (37) and (38). This finding has been employed in deriving the BCM for generalized beam shapes [1].

5 BCM Energy Formulation for Initially Straight Variable Cross-Section Beams

In this section, we employ the results from the previous two sections to present an energy formulation associated with the BCM for a variable cross-section beam. One of the questions raised at the end of Sec. 3 was how to determine the truncation of the transverse load-displacement (Eq. (24)), axial geometric constraint (Eq. (25)), and strain energy (Eq. (26)) expressions, all of which are expressed in the form of infinite series in the axial load $\boldsymbol{f_{x1}}$. Observation 3 from the previous section helps provide an answer. Since these three expressions are all inter-related, their truncation should be such that the expressions remain consistent in terms of PVW even after truncation. Maintaining this consistency is important because ultimately we plan to use only the truncated strain energy of a generalized beam in deriving the load-displacement relations for more complex flexure mechanisms constructed from multiple such beams.

It has been identified analytically as well as experimentally [1–4] that terms up to the first power in $\boldsymbol{f_{x1}}$ have to be retained both in the constraint expression to capture the kinematic and elastokinematic effects, and in the transverse load-displacement expression to capture the elastic and load-stiffening effects. Based on these requirements, a consistent BCM, comprising transverse load-displacement, axial constraint, and strain energy relations, that captures elastic stiffness, load-stiffening, kinematic, and elastokinematic effects is given by

$$\begin{aligned} \begin{Bmatrix} \boldsymbol{f_{y1}} \\ \boldsymbol{m_{z1}} \end{Bmatrix} &= \begin{bmatrix} k_{11}^{(0)} & k_{12}^{(0)} \\ k_{12}^{(0)} & k_{22}^{(0)} \end{bmatrix} \begin{Bmatrix} u_{y1} \\ \theta_{z1} \end{Bmatrix} + \boldsymbol{f_{x1}} \begin{bmatrix} k_{11}^{(1)} & k_{12}^{(1)} \\ k_{12}^{(1)} & k_{22}^{(1)} \end{bmatrix} \begin{Bmatrix} u_{y1} \\ \theta_{z1} \end{Bmatrix} \\ &\quad + \boldsymbol{f_{x1}^2} \begin{bmatrix} k_{11}^{(2)} & k_{12}^{(2)} \\ k_{12}^{(2)} & k_{22}^{(2)} \end{bmatrix} \begin{Bmatrix} u_{y1} \\ \theta_{z1} \end{Bmatrix} \end{aligned} \tag{39}$$

$$\begin{aligned} u_{x1} &= u_{x1}^{(e)} + \{u_{y1} \quad \theta_{z1}\} \begin{bmatrix} g_{11}^{(0)} & g_{12}^{(0)} \\ g_{12}^{(0)} & g_{22}^{(0)} \end{bmatrix} \begin{Bmatrix} u_{y1} \\ \theta_{z1} \end{Bmatrix} \\ &\quad + \boldsymbol{f_{x1}} \{u_{y1} \quad \theta_{z1}\} \begin{bmatrix} g_{11}^{(1)} & g_{12}^{(1)} \\ g_{12}^{(1)} & g_{22}^{(1)} \end{bmatrix} \begin{Bmatrix} u_{x1} \\ \theta_{z1} \end{Bmatrix} \end{aligned} \tag{40}$$

$$\begin{aligned} v &= \frac{1}{2} k_{33} u_{x1}^{(e)^2} + \frac{1}{2} \{u_{y1} \quad \theta_{z1}\} \begin{bmatrix} v_{11}^{(0)} & v_{12}^{(0)} \\ v_{12}^{(0)} & v_{22}^{(0)} \end{bmatrix} \begin{Bmatrix} u_{y1} \\ \theta_{z1} \end{Bmatrix} \\ &\quad + \frac{1}{2} \boldsymbol{f_{x1}^2} \{u_{y1} \quad \theta_{z1}\} \begin{bmatrix} v_{11}^{(2)} & v_{12}^{(2)} \\ v_{12}^{(2)} & v_{22}^{(2)} \end{bmatrix} \begin{Bmatrix} u_{y1} \\ \theta_{z1} \end{Bmatrix} \end{aligned} \tag{41}$$

subject to the following relations between the beam characteristic coefficients:

$$k_{\beta\lambda}^{(0)} = v_{\beta\lambda}^{(0)}, \quad g_{\beta\gamma}^{(0)} = -\tfrac{1}{2} k_{\beta\gamma}^{(1)}, \quad g_{\beta\gamma}^{(1)} = v_{\beta\lambda}^{(2)} = -k_{\beta\gamma}^{(2)} \tag{42}$$

Note that, originally, we did not include the second-power term in $\boldsymbol{f_{x1}}$ in the BCM [1,2] because its contribution was found to be practically negligible. However, based on the new insight gained in the previous section regarding consistency in the formulation, it becomes essential to include this second-power $\boldsymbol{f_{x1}}$ term in the transverse load-displacement and strain energy expressions if we are to correctly retain the elastokinematic effect (first-power $\boldsymbol{f_{x1}}$ term) in the constraint expression.

To employ the above results in an energy method such as PVW, we need to know the strain energy and geometric constraint expressions for any constituent flexure beams in terms of displacements only. However, in their present forms, both these expressions exhibit the presence of the axial load $\boldsymbol{f_{x1}}$. Therefore, further modification of these two expressions is carried out by making the logical substitution $\boldsymbol{f_{x1}} = k_{33} u_{x1}^{(e)}$ to yield

$$\begin{aligned} v &= \frac{1}{2} k_{33} u_{x1}^{(e)^2} \left(1 + k_{33} \{u_{y1} \quad \theta_{z1}\} \begin{bmatrix} v_{11}^{(2)} & v_{12}^{(2)} \\ v_{12}^{(2)} & v_{22}^{(2)} \end{bmatrix} \begin{Bmatrix} u_{y1} \\ \theta_{z1} \end{Bmatrix} \right) \\ &\quad + \frac{1}{2} \{u_{y1} \quad \theta_{z1}\} \begin{bmatrix} v_{11}^{(0)} & v_{12}^{(0)} \\ v_{12}^{(0)} & v_{22}^{(0)} \end{bmatrix} \begin{Bmatrix} u_{y1} \\ \theta_{z1} \end{Bmatrix} \end{aligned}$$

$$\begin{aligned} u_{x1} &= u_{x1}^{(e)} \left(1 + k_{33} \{u_{y1} \quad \theta_{z1}\} \begin{bmatrix} g_{11}^{(1)} & g_{12}^{(1)} \\ g_{12}^{(1)} & g_{22}^{(1)} \end{bmatrix} \begin{Bmatrix} u_{x1} \\ \theta_{z1} \end{Bmatrix} \right) \\ &\quad + \{u_{y1} \quad \theta_{z1}\} \begin{bmatrix} g_{11}^{(0)} & g_{12}^{(0)} \\ g_{12}^{(0)} & g_{22}^{(0)} \end{bmatrix} \begin{Bmatrix} u_{y1} \\ \theta_{z1} \end{Bmatrix} \end{aligned}$$

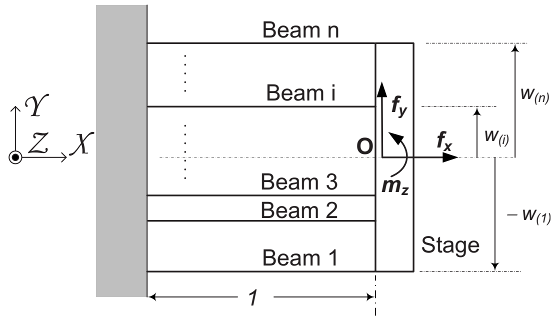

Fig. 3 Multibeam parallelogram flexure

Now, these expressions are in the desirable form, i.e., free of any load terms. The independent displacement variables in this case are $u_{x1}^{(e)}$, u_{y1}, and θ_{z1}; and u_{x1} is a dependent displacement coordinate related to the former three via the second of the above two equations. Alternatively, the constraint equation may be substituted into the strain energy expression while employing relation (42) to yield

$$v=\frac{1}{2}k_{33}\frac{\left(u_{x1}+\frac{1}{2}\{u_{y1}\quad\theta_{z1}\}\begin{bmatrix}k_{11}^{(1)} & k_{12}^{(1)}\\ k_{12}^{(1)} & k_{22}^{(1)}\end{bmatrix}\begin{Bmatrix}u_{y1}\\ \theta_{z1}\end{Bmatrix}\right)^2}{\left(1-k_{33}\{u_{y1}\quad\theta_{z1}\}\begin{bmatrix}k_{11}^{(2)} & k_{12}^{(2)}\\ k_{12}^{(2)} & k_{22}^{(2)}\end{bmatrix}\begin{Bmatrix}u_{x1}\\ \theta_{z1}\end{Bmatrix}\right)}+\frac{1}{2}\{u_{y1}\quad\theta_{z1}\}\begin{bmatrix}k_{11}^{(0)} & k_{12}^{(0)}\\ k_{12}^{(0)} & k_{22}^{(0)}\end{bmatrix}\begin{Bmatrix}u_{y1}\\ \theta_{z1}\end{Bmatrix} \quad (43)$$

This is the final nonlinear expression for strain energy that is consistent with the BCM. In this form, the strain energy may be used directly in an energy-based analysis of multibeam flexure mechanisms, without the need for an additional constraint expression. Since the constraint is implicit here, u_{x1}, u_{y1}, and θ_{z1} represent three independent displacement variables.

6 Multibeam Parallelogram Flexure Analysis Using the BCM Energy Formulation

A multibeam parallelogram flexure mechanism is shown in Fig. 3. A rigid stage is connected to the ground via parallel and identical beams, not necessarily uniform in thickness, numbered 1 through n. External loads $\boldsymbol{f_x}$, $\boldsymbol{f_y}$, and $\boldsymbol{m_z}$, normalized as per the previously described scheme, act at point O on the rigid stage. A reference line, passing through O and parallel to the beams, is used to specify the location of the ith beam via the geometric parameter w_i measured along the positive Y axis. The spacing between the beams is arbitrary. The normalized displacements of point O, under the given loads, are denoted by u_x, u_y, and θ_z (not shown in the figure). It is physically obvious that the Y direction represents a DoF, while the axial direction X and transverse rotational direction Θ_Z represent DoC given their high stiffness.

The multibeam parallelogram flexure module allows the use of thinner beams that leads to a low DoF stiffness without compromising DoC stiffness. This ensures a larger DoF motion range along with good DoC load bearing capacity [4,8,9]. Consequently, one would like to study the effect of the number of beams and their spacing on stiffness and error motion behavior. This necessitates the determination of the stage displacements in terms of the three externally applied loads. A direct analysis of this system would require the creation of free body diagrams for each beam, explicitly identifying its end loads. The end load-displacement relations for each beam provide $3n$ constitutive relations, while another three equations are obtained from the load equilibrium of the stage in its displaced configuration. These $3(n+1)$ equations have to be solved simultaneously for the $3n$ unknown internal end loads and the three displacements of the motion stage (u_x, u_y, and θ_z). Even though the $3n$ internal end loads are of no interest, they have to be determined in this direct analysis. Obviously, the complexity associated with solving $3(n+1)$ equations grows with increasing number of beams.

Instead, an energy-based approach for determining the load-displacement relations for the multibeam parallelogram flexure turns out to be far more efficient. We first identify the geometric compatibility conditions in this case by expressing the end displacements of each beam in terms of the stage displacements. Since a physical understanding of the system as well as previous analytical results [2,4] show that the stage angle θ_z is very small ($\sim 10^{-3}$), the small angle approximations $\cos\theta_z=1$ and $\sin\theta_z=\theta_z$ are well justified. Thus, the end displacements for the ith beam are given by

$$u_{x1(i)}\approx u_x-w_{(i)}\theta_z$$

$$u_{y1(i)}\approx u_y \quad (44)$$

$$\theta_{z1(i)}\approx\theta_z$$

Next, using Eq. (43), the strain energy for the ith beam is given by

$$v_{(i)}=\frac{1}{2}k_{33}\frac{\left(u_x-w_{(i)}\theta_z+\frac{1}{2}\{u_y\quad\theta_z\}\begin{bmatrix}k_{11}^{(1)} & k_{12}^{(1)}\\ k_{12}^{(1)} & k_{22}^{(1)}\end{bmatrix}\begin{Bmatrix}u_y\\ \theta_z\end{Bmatrix}\right)^2}{\left(1-k_{33}\{u_y\quad\theta_z\}\begin{bmatrix}k_{11}^{(2)} & k_{12}^{(2)}\\ k_{12}^{(2)} & k_{22}^{(2)}\end{bmatrix}\begin{Bmatrix}u_y\\ \theta_z\end{Bmatrix}\right)}+\frac{1}{2}\{u_y\quad\theta_z\}\begin{bmatrix}k_{11}^{(0)} & k_{12}^{(0)}\\ k_{12}^{(0)} & k_{22}^{(0)}\end{bmatrix}\begin{Bmatrix}u_y\\ \theta_z\end{Bmatrix} \quad (45)$$

The total strain energy of the system is simply the sum of the strain energies of all the beams:

$$v=\frac{1}{2}k_{33}\frac{\sum_{i=1}^{n}\left(u_x-w_{(i)}\theta_z+\frac{1}{2}\{k_{11}^{(1)}u_y^2+2k_{12}^{(1)}u_y\theta_z+k_{22}^{(1)}\theta_z^2\}\right)^2}{(1-k_{33}\{k_{11}^{(2)}u_y^2+2k_{12}^{(2)}u_y\theta_z+k_{22}^{(2)}\theta_z^2\})}+\frac{1}{2}n\{k_{11}^{(0)}u_y^2+2k_{12}^{(0)}u_y\theta_z+k_{22}^{(0)}\theta_z^2\} \quad (46)$$

Applying the PVW, the variation in strain energy in response to virtual displacements δu_x, δu_y, and $\delta\theta_z$ may be equated to the virtual work done by external forces. In the resulting equation, the coefficients of each of these mutually independent virtual displacements may be identically set to zero. This results in the following three relations, where the first one is used to simplify the subsequent two:

$$\boldsymbol{f_x}=nk_{33}\frac{\left(u_x+\frac{1}{2}\{k_{11}^{(1)}u_y^2+2k_{12}^{(1)}u_y\theta_z+k_{22}^{(1)}\theta_z^2\}\right)-\left(\frac{1}{n}\sum_{i=1}^{n}w_{(i)}\right)\theta_z}{(1-k_{33}\{k_{11}^{(2)}u_y^2+2k_{12}^{(2)}u_y\theta_z+k_{22}^{(2)}\theta_z^2\})} \quad (47)$$

$$\boldsymbol{f_y}=k_{33}\sum_{i=1}^{n}\left\{\frac{\boldsymbol{f_x}}{nk_{33}}+\frac{\left(\frac{1}{n}\sum_{i=1}^{n}w_{(i)}-w_{(i)}\right)\theta_z}{(1-k_{33}\{k_{11}^{(2)}u_y^2+2k_{12}^{(2)}u_y\theta_z+k_{22}^{(2)}\theta_z^2\})}\right\}\times(k_{11}^{(1)}u_y+k_{12}^{(1)}\theta_z)$$
$$+k_{33}^2\sum_{i=1}^{n}\left\{\frac{\boldsymbol{f_x}}{nk_{33}}+\frac{\left(\frac{1}{n}\sum_{i=1}^{n}w_{(i)}-w_{(i)}\right)\theta_z}{(1-k_{33}\{k_{11}^{(2)}u_y^2+2k_{12}^{(2)}u_y\theta_z+k_{22}^{(2)}\theta_z^2\})}\right\}^2$$

$$\times(k_{11}^{(2)}u_y + k_{12}^{(2)}\theta_z) + n(k_{11}^{(0)}u_y + k_{12}^{(0)}\theta_z) \tag{48}$$

$$\begin{aligned}\boldsymbol{m_z} = k_{33}\sum_{i=1}^{n}\Bigg[\Bigg[\Bigg\{\frac{\boldsymbol{f_x}}{nk_{33}} + \frac{\left(\frac{1}{n}\sum_{i=1}^{n} w_{(i)} - w_{(i)}\right)\theta_z}{(1 - k_{33}\{k_{11}^{(2)}u_y^2 + 2k_{12}^{(2)}u_y\theta_z + k_{22}^{(2)}\theta_z^2\})}\Bigg\} \\ \times(-w_{(i)} + k_{12}^{(1)}u_y + k_{22}^{(1)}\theta_z)\Bigg] \\ + k_{33}^2\sum_{i=1}^{n}\Bigg\{\frac{\boldsymbol{f_x}}{nk_{33}} \\ + \frac{\left(\frac{1}{n}\sum_{i=1}^{n} w_{(i)} - w_{(i)}\right)\theta_z}{(1 - k_{33}\{k_{11}^{(2)}u_y^2 + 2k_{12}^{(2)}u_y\theta_z + k_{22}^{(2)}\theta_z^2\})}\Bigg\}^2 (k_{12}^{(2)}u_y + k_{22}^{(2)}\theta_z) \\ + n(k_{12}^{(0)}u_y + k_{22}^{(0)}\theta_z)\end{aligned} \tag{49}$$

For a DoF motion range $u_y \sim 0.1$, Eq. (47) may be simplified by recognizing that $\theta_z \ll u_y$ to yield the axial-direction displacement:

$$u_x = \frac{\boldsymbol{f_x}}{nk_{33}} - \frac{1}{2}k_{11}^{(1)}u_y^2 - \frac{\boldsymbol{f_x}}{n}k_{11}^{(2)}u_y^2 \tag{50}$$

Clearly, the first term above is a purely elastic term arising from an axial stretching of the beams. The second term is a kinematic term, which is independent of the number of beams. The final term is an elastokinematic term. Similarly, Eq. (48) may be simplified to the following form:

$$\boldsymbol{f_y} = \left(nk_{11}^{(0)} + \boldsymbol{f_x}k_{11}^{(1)} + \frac{1}{n}\boldsymbol{f_x}^2k_{11}^{(2)}\right)u_y \tag{51}$$

Here, the first term may be identified to be the elastic stiffness term, and the second term is a load-stiffening term, which is seen to be independent of the number of beams. The consistency of the energy formulation, described above, dictates that if the elastokinematic term is captured in Eq. (50), the third term (second power in $\boldsymbol{f_x}$) will appear in Eq. (51). At this final stage, one may choose to drop this second-power term because its contribution is practically negligible for typical beam shapes and load ranges of interest.

Similarly, Eq. (49) may be simplified as follows:

$$\theta_z = \frac{\left[\boldsymbol{m_z} + \frac{\boldsymbol{f_x}}{n}\left(\sum_{i=1}^{n} w_{(i)}\right) - \left(nk_{12}^{(0)} + \boldsymbol{f_x}k_{12}^{(1)} + \frac{\boldsymbol{f_x}^2}{n}k_{12}^{(2)}\right)u_y\right]\left(\frac{1}{k_{33}} - k_{11}^{(2)}u_y^2\right)}{\left[\sum_{i=1}^{n} w_{(i)}^2 - \frac{1}{n}\left\{\left(\sum_{i=1}^{n} w_{(i)}\right)^2\right\} + \left(\frac{1}{k_{33}} - k_{11}^{(2)}u_y^2\right)\left(nk_{22}^{(0)} + k_{22}^{(1)}\boldsymbol{f_x} + \frac{k_{22}^{(2)}\boldsymbol{f_x}^2}{n}\right)\right]}$$

Furthermore, recognizing that k_{33} is several orders of magnitude larger than all the other stiffness coefficients and that the second-power terms in $\boldsymbol{f_x}$ may be neglected, the above relation reduces to

$$\theta_z \approx \frac{\left[\boldsymbol{m_z} + \frac{\boldsymbol{f_x}}{n}\left(\sum_{i=1}^{n} w_{(i)}\right) - (nk_{12}^{(0)} + \boldsymbol{f_x}k_{12}^{(1)})u_y\right]\left(\frac{1}{k_{33}} - k_{11}^{(2)}u_y^2\right)}{\left[\sum_{i=1}^{n} w_{(i)}^2 - \frac{1}{n}\left\{\left(\sum_{i=1}^{n} w_{(i)}\right)^2\right\}\right]} \tag{52}$$

Next, the accuracy of the above closed-form parametric analytical results is corroborated via nonlinear finite element analysis (FEA) carried out in ANSYS. A seven-beam parallelogram flexure is selected for this FEA study, with the beam locations w_i arbitrarily chosen with respect to a reference X axis that passes through the center of the stage. Each simple beam (initially straight and uniform in thickness) is 5 mm in thickness, 50 mm in height, and 250 mm in length; the latter serves to normalize all other displacements and length dimensions. The normalized values of the w_i selected are −0.6, −0.45, −0.25, −0.1, 0.2, 0.35, and 0.6. BEAM4 elements are used for meshing, and the consistent matrix and large displacement (NLGEOM) options are turned on to capture all nonlinearities in the problem. A Young's modulus of 210,000 N/mm^2 and Poisson's ratio of 0.3 are used assuming the material to be steel. The normalized DoF displacement u_y is varied from −0.12 to 0.12. The parasitic axial displacement of the stage u_x (Fig. 4) is determined while keeping $\boldsymbol{f_x} = \boldsymbol{m_x} = 0$. The parasitic rotation of the stage θ_z (Fig. 5) and the X direction stiffness (Fig. 6) are determined while setting the normalized axial force $\boldsymbol{f_x}$ to 1 and $\boldsymbol{m_x}$ and to 0.

These FEA results for the seven-beam parallelogram are in agreement with the BCM predictions (Eqs. (50)–(52)), within a 5% error. In general, this flexure module exhibits constraint characteristics very similar to the two-beam parallelogram flexure module. Its key advantage is a 3.5 times greater X DoC stiffness

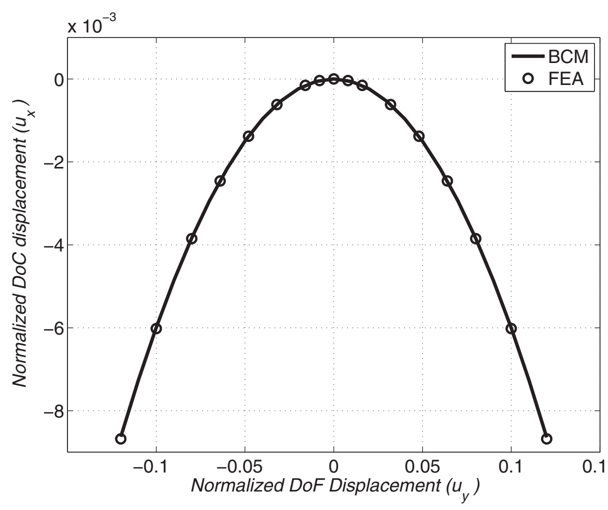

Fig. 4 Parasitic axial displacement u_x (DoC) versus transverse displacement u_y (DoF)

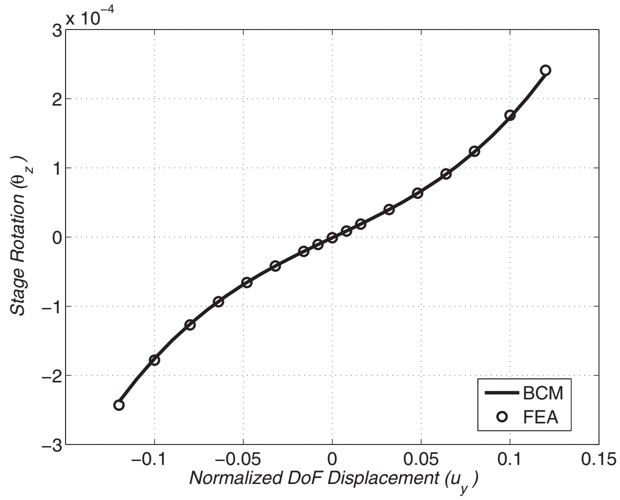

Fig. 5 Parasitic stage rotation θ_z (DoC) versus transverse displacement u_y (DoF)

(and therefore load bearing capacity) without compromising the motion Y DoF motion range and adversely affecting the X and Θ_Z DoC parasitic errors.

This example shows that once a consistent BCM energy formulation has been derived, the use of energy methods considerably reduces the mathematical complexity in the analysis of increasingly sophisticated flexure mechanisms. The above procedure is relatively independent of the number of beams chosen or the shapes of the individual beams, as long as the strain energy associated with each beam is accounted for correctly.

7 BCM Energy Formulation for Initially Slanted and Curved Beams

We next consider a uniform-thickness beam with an arbitrary initial angle α and an arbitrary but constant curvature κ. Figure 7 shows such a beam with generalized end loads and end displacements along the X-Y-Z coordinate frame. All physical quantities are normalized as per the scheme described previously.

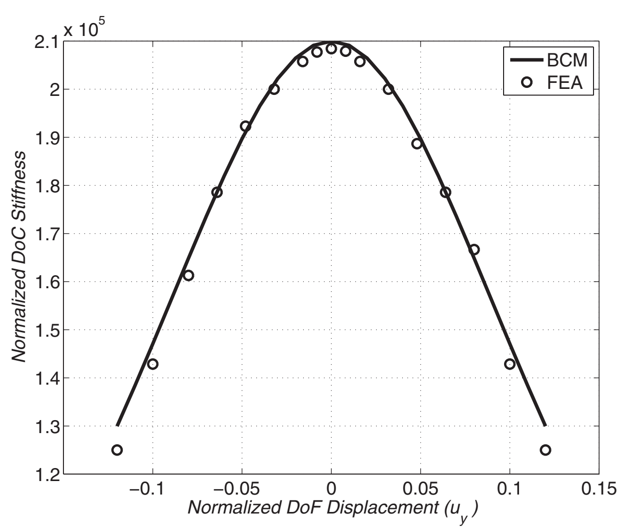

Fig. 6 Axial stiffness (DoC) versus transverse displacement u_y (DoF)

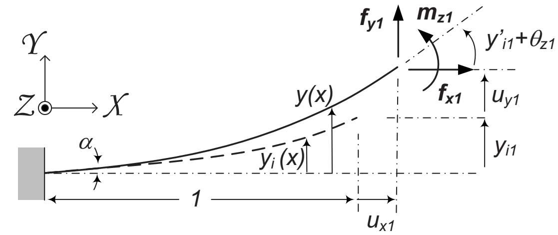

Fig. 7 Initially slanted and curved beams

The initial (unloaded and undeformed) beam configuration is denoted by $y_i(x)$, the final (loaded and deformed) beam configuration is given by $y(x)$, and the beam deformation in the Y direction is given by $u_y(x)$, where

$$y_i(x) = \alpha x + \frac{\kappa}{2}x^2 \ \text{ and } \ y(x) = y_i(x) + u_y(x) \tag{53}$$

Along the previous lines, the beam governing equation may be shown to be

$$\begin{aligned} y''(x) - \kappa &= \boldsymbol{m_{z1}} + \boldsymbol{f_{y1}}(1 + u_{x1} - x) - \boldsymbol{f_{x1}}(y_1 - y(x)) \\ &\Rightarrow y^{iv}(x) = \boldsymbol{f_{x1}} y''(x) \end{aligned} \tag{54}$$

It is important to note that for the curvature linearization assumption to be valid in the above beam governing equation, the initial slope α and the normalized curvature κ have to be of the order of 0.1 or less. This equation, along with boundary conditions $u_y(0)=0$, $u_y'(0)=0$, $u_y(1)=u_{y1}$, and $u_y'(1)=\theta_{z1}$, may be solved in closed form to determine $u_y(x)$. This solution is substituted in Eq. (10) to derive the following strain energy expression:

$$\begin{aligned} v = \frac{1}{2}k_{33}(u_{x1}^{(e)})^2 + \frac{1}{2}\{u_{y1} \quad \theta_{z1}\} \begin{bmatrix} v_{11}(\boldsymbol{f_{x1}}) & v_{12}(\boldsymbol{f_{x1}}) \\ v_{21}(\boldsymbol{f_{x1}}) & v_{22}(\boldsymbol{f_{x1}}) \end{bmatrix} \begin{Bmatrix} u_{y1} \\ \theta_{z1} \end{Bmatrix} \\ + v_{44}\left(\theta_{z1} + \frac{\kappa}{2}\right)\frac{\kappa}{2} \end{aligned} \tag{55}$$

where k_{33}, v_{11}, v_{12}, and v_{22} are the same as in Eq. (17), and

$$\begin{aligned} v_{44} = &\frac{-(\cosh \boldsymbol{r} - 1)}{2(\boldsymbol{r} \sinh \boldsymbol{r} - 2 \cosh \boldsymbol{r} + 2)^2} \\ &\times \{\boldsymbol{r}^4(1 + \cosh \boldsymbol{r}) + \boldsymbol{r}^3 \sinh \boldsymbol{r}(\cosh \boldsymbol{r} - 3)\} \\ &\times \{4\boldsymbol{r}^2(2 \cosh \boldsymbol{r}+1) + 16(\cosh \boldsymbol{r} - 1) - 20\boldsymbol{r} \sinh \boldsymbol{r}\} \end{aligned}$$

The above transcendental functions may be expanded to an infinite series in $\boldsymbol{f_{x1}}$ ($\triangleq \boldsymbol{r}^2$), and the third power and higher terms may be truncated to yield the following compact form:

$$\begin{aligned} v = &\frac{1}{2}k_{33}(u_{x1}^{(e)})^2 + \frac{1}{2}\{u_{y1} \quad \theta_{z1}\} \begin{bmatrix} 12 & -6 \\ -6 & 4 \end{bmatrix} \begin{Bmatrix} u_{y1} \\ \theta_{z1} \end{Bmatrix} \\ &+ \frac{1}{2}\boldsymbol{f_{x1}}^2\{u_{y1} \quad \theta_{z1}\} \begin{bmatrix} \frac{1}{700} & -\frac{1}{1400} \\ -\frac{1}{1400} & \frac{11}{6300} \end{bmatrix} \begin{Bmatrix} u_{y1} \\ \theta_{z1} \end{Bmatrix} + \boldsymbol{f_{x1}}^2 \frac{\kappa \theta_{z1}}{720} \\ &+ \boldsymbol{f_{x1}}^2 \frac{\kappa^2}{1440} \end{aligned} \tag{56}$$

The last two terms in this strain energy expression for an initially slanted and curved beam are new compared to Eq. (18) for an initially straight beam. Separately, the geometric constraint expression may be derived from

$$\int_0^{1+u_{x1}^{(e)}} \left\{ 1 + \frac{1}{2}(y_i'(x))^2 \right\} dx = \int_0^{1+u_{x1}} \left\{ 1 + \frac{1}{2}(u_y'(x) + y_i'(x))^2 \right\} dx \tag{57}$$

to yield a closed-form expression for the axial end displacement u_{x1}. The resulting expression may be expanded and truncated to retain up to second-power terms in $\boldsymbol{f_{x1}}$ as follows:

$$u_{x1} = u_{x1}^{(e)} + \{u_{y1} \quad \theta_{z1}\} \begin{bmatrix} -\frac{3}{5} & \frac{1}{20} \\ \frac{1}{20} & -\frac{1}{15} \end{bmatrix} \begin{Bmatrix} u_{y1} \\ \theta_{z1} \end{Bmatrix} + \boldsymbol{f_{x1}} \{u_{y1} \quad \theta_{z1}\} \begin{bmatrix} \frac{1}{700} & -\frac{1}{1400} \\ -\frac{1}{1400} & \frac{11}{6300} \end{bmatrix} \begin{Bmatrix} u_{y1} \\ \theta_{z1} \end{Bmatrix} - \left(\alpha + \frac{\kappa}{2}\right) u_{y1} - \frac{\kappa}{12}\theta_{z1} + \boldsymbol{f_{x1}} \frac{\kappa}{360}\theta_{z1} + \boldsymbol{f_{x1}} \frac{\kappa^2}{720} \tag{58}$$

One may notice similarities in the energy and constraint coefficients of Eqs. (56) and (58), respectively. The reason for this can be traced back to the same arguments as were provided for an initially straight beam in Sec. 4. Furthermore, setting $\alpha=\kappa=0$ reduces the above equations to those for an initially straight beam, as expected. It is interesting to note the absence of an initial beam slant angle α in the strain energy expression (56). This can be justified based on the constraint expression (58), where α is present only in the kinematic terms and not in any elastokinematic terms. Since the kinematic terms arise purely from geometry and not elastic deformation, α does not appear in the strain energy expression. The last two terms of the constraint expression, which are dependent on curvature κ, represent elastokinematic deformation and can be seen to correspond with the last two terms in the strain energy expression.

As in the case of an initially straight beam, both the constraint and strain energy expressions above have an explicit dependence on the axial load $\boldsymbol{f_{x1}}$. Employing the same arguments as presented at the end of Sec. 5, $\boldsymbol{f_{x1}}$ may be first replaced with $k_{33}u_{x1}^{(e)}$ in these two expressions, and $u_{x1}^{(e)}$ from the resulting constraint expression may be substituted in the resulting energy expression to yield

$$v = \frac{1}{2}k_{33} \frac{\left(u_{x1} - \{u_{y1} \quad \theta_{z1}\} \begin{bmatrix} -\frac{3}{5} & \frac{1}{20} \\ \frac{1}{20} & -\frac{1}{15} \end{bmatrix} \begin{Bmatrix} u_{y1} \\ \theta_{z1} \end{Bmatrix} + \left(\alpha + \frac{\kappa}{2}\right) u_{y1} + \frac{\kappa}{12}\theta_{z1} \right)^2}{\left(1 + k_{33}\{u_{y1} \quad \theta_{z1}\} \begin{bmatrix} \frac{1}{700} & -\frac{1}{1400} \\ -\frac{1}{1400} & \frac{11}{6300} \end{bmatrix} \begin{Bmatrix} u_{y1} \\ \theta_{z1} \end{Bmatrix} + k_{33}\frac{\kappa\theta_{z1}}{360} + k_{33}\frac{\kappa^2}{720} \right)} + \frac{1}{2}\{u_{y1} \quad \theta_{z1}\} \begin{bmatrix} 12 & -6 \\ -6 & 4 \end{bmatrix} \begin{Bmatrix} u_{y1} \\ \theta_{z1} \end{Bmatrix} \tag{59}$$

This is the final nonlinear strain energy expression for an initially slanted and curved beam that may be used in energy methods, with u_{x1}, u_{y1}, and θ_{z1} as the three independent displacement variables. It should be noted that while the above derivation was carried out for a uniform-thickness beam, one may easily generalize it to any variable cross-section beam using the procedure outlined in Sec. 3. Upon such generalization, the numerical values of the energy and constraint coefficients above will be replaced by the generic symbols v and g, respectively.

8 Conclusion

In the past, the BCM has been shown to be a dimensionless, generalized, closed-form, and parametric mathematical model that accurately captures the constraint characteristics of flexure mechanisms. These constraint characteristics are based on the stiffness and error motions in flexure elements and mechanisms and are strongly dependent on geometric nonlinearities. However, the application of the BCM to more complex flexure mechanisms has proven to be tedious due to the involvement of internal loads, which are not directly relevant to the desired load-displacement relations.

The primary contribution of this paper is to provide a nonlinear strain energy formulation of the BCM so that it may be employed in energy methods, such as the principle of virtual work, to efficiently derive the nonlinear load-displacement relations for complex flexure mechanisms. Energy methods avoid internal loads, thus greatly reducing mathematical complexity. We believe that this ability to accurately and quickly analyze complex flexure mechanisms is a critical first step toward their constraint-based synthesis and optimization.

This research was supported in part by a National Science Foundation grant (Grant No. CMMI 0846738).

References

[1] Awtar, S., and Sen, S., 2010, "A Generalized Constraint Model for Two-Dimensional Beam Flexures: Non-Linear Load-Displacement Formulation," ASME J. Mech. Des. **132**, p. 081008.
[2] Awtar, S., Slocum, A. H., and Sevincer, E., 2007, "Characteristics of Beam-Based Flexure Modules," ASME J. Mech. Des., **129**(6), pp. 625–639.
[3] Awtar, S., and Slocum, A. H., 2007, "Constraint-Based Design of Parallel Kinematic XY Flexure Mechanisms," ASME J. Mech. Des., **129**(8), pp. 816–830.
[4] Awtar, S., and Sevincer, E., 2006, "Elastic Averaging in Flexure Mechanisms: A Multi-Parallelogram Flexure Case-Study," Proceedings of ASME IDETC/CIE 2006, Philadelphia, PA, Paper No. 99752.
[5] Tauchert, T. R., 1974, *Energy Principles in Structural Mechanics*, McGraw-Hill, New York.
[6] Hodges, D. H., 1984, "Proper Definition of Curvature in Nonlinear Beam Kinematics," AIAA J., **22**(12), pp. 1825–1827.
[7] Mayo, J., and Dominguez, J., 1992, "Geometrically Nonlinear Coupling Between Axial and Flexural Modes of Deformation of Multibody Systems," Winter Annual Meeting of ASME: Dynamics of Flexible Multibody Systems: Theory and Experiments, Anaheim, CA, AMD-v.141, DSC-v.37, pp 95–103.
[8] Bonin, W. A., 2001, "Microactuator Suspension With Multiple Narrow Beams," U.S. Patent No. 6,282,066.
[9] Trease, B. P., Moon, Y.-M., and Kota, S., 2005, "Design of Large Displacement Compliant Joints," ASME J. Mech. Des., **127**(4), pp. 788–798.